Available online at www.sciencedirect.com
SCIENCE DIRECT®
Journal of Sound and Vibration 290 (2006) 465–489
JOURNAL OF SOUND AND VIBRATION
www.elsevier.com/locate/jsvi

Vibration of shear deformable plates with variable thickness — first-order and higher-order analyses

I. Shufrin, M. Eisenberger*

Faculty of Civil and Environmental Engineering, Technion-Israel Institute of Technology, Technion City, Haifa 32000, Israel

Received 9 December 2003; received in revised form 1 April 2005; accepted 4 April 2005
Available online 11 July 2005

Abstract

This work presents accurate numerical calculations of the natural frequencies for elastic rectangular plates of variable thickness with various combinations of boundary conditions. The thickness variation in one or two directions of the plate is taken in polynomial form. The first-order shear deformation plate theory of Mindlin and the higher-order shear deformation plate theory of Reddy have been applied to the plate analysis. The governing equations and the boundary conditions are derived using the dynamic version of the principle of minimum of the Lagrangian function. The solution is obtained by the extended Kantorovich method. This approach is combined with the exact element method for the vibration analysis of members with variable flexural rigidity, which provides for the derivation of the exact dynamic stiffness matrix of varying cross-sections strips. The large number of numerical examples demonstrates the applicability and versatility of the present method. The results obtained by both shear deformation theories are compared with those obtained by the classical thin plate theory and with published results.

1. Introduction

Plate elements with varying thickness are used in civil, mechanical, aeronautical and marine structures. The consideration of free vibration of such plates is essential to have an efficient and

*Corresponding author. Tel.: +972 4 8292413; fax: +972 4 8295697.
E-mail address: cvrmosh@tx.technion.ac.il (M. Eisenberger).

0022-460X/$ - see front matter © 2005 Elsevier Ltd. All rights reserved.
doi:10.1016/j.jsv.2005.04.003

reliable design. The use of variable thickness helps to reduce the weight of structural elements and improve the utilization of the material.

The classical Kirchhoff thin plate theory (CPT) is usually used to carry out vibration analysis of rectangular plates. CPT assumptions are satisfactory for low mode computation of truly thin plate, but they can lead to inaccuracy in higher modes calculation or when the ratio of thickness to the dimension of plate is relatively large. This is because the effects of rotary inertia, which is neglected in most references, and the transverse shear deformations, which cannot be considered in the Kirchhoff theory, become significant in thick plates. For that reason a number of shear deformation plate theories were developed. The simplest one is the first-order shear deformation plate theory (FOPT) that is famous as the Reissner–Mindlin theory. This approach extends the kinematic assumptions of the CPT by releasing the restriction on the angle of shearing deformations [1,2]. The transverse shear strain is assumed to be constant through the thickness of the plate, and a shear correction factor is introduced to correct the discrepancy between the actual transverse shear stress distribution and those computed using the kinematic relations of this theory. The shear correction factors depend not only on geometric parameters, but also on the loading and boundary conditions of the plate. Second and higher-order shear deformation plate theories (HOPT) [1,3,4] use higher-order polynomials in the expansion of the displacement components through the thickness of the plate. According to the assumptions of HOPT the restriction on warping of the cross-section is relaxed, and allows variation in the thickness direction of the plate. Unlike the FOPT, the HOPT requires no shear correction factors.

By using various kinds of analytical and numerical methods, many researchers have extensively studied free vibration of rectangular thick plates with constant thickness according to HOPT [3–6] and FOPT [7–9] approaches and rectangular thin plate with variable thickness [10,11]. However, the analysis of rectangular thick plates with non-uniform thickness has attracted less attention. Mikami and Yoshimura [12] have applied the collocation method with orthogonal polynomials to calculate the natural frequencies for rectangular Reissner–Mindlin plates with linear thickness variation. Al-Kaabi and Aksu [14] have presented a method based on a variational principle in conjunction with finite difference technique for analysis of Reissner–Mindlin plates of linearly [13] and parabolically [14] varying thickness. Based on the FOPT, Mizusawa [15] has employed the spline strip method for computation of natural frequencies for the tapered rectangular plates. In all these studies, only plates with two opposite simply supported edges perpendicular to direction of thickness variation are considered. Cheung and Zhou [16] have used the Rayleigh–Ritz method for free vibration solution of rectangular Reissner–Mindlin plates with variable thickness and different boundary conditions. The variation of the thickness in their work is described by a power function of the Cartesian coordinates. To the best of our knowledge, no solutions have been given for the problem of free vibration of rectangular plates with variable thickness based on the higher-order shear deformation plate theories.

The object of the present work is to give highly accurate solutions for the free vibration problem of rectangular plates with any general polynomial variation of the thickness, including the effect of the shear deformations and rotary inertia. The dynamic version of the principle of minimum of the Lagrangian function is adopted in the derivation of the governing equations and the boundary conditions, for the Reissner–Mindlin FOPT and the HOPT of Reddy. The solution is based on

the extended Kantorovich method [9,17,18]. According to this approach the solution is assumed to be separable in the directions of the plate edges. Then, the solution in one direction, x for example, is specified a priori, and the solution in the y direction is determined by solving an ordinary differential equation derived from the associated variational process with appropriate boundary conditions. In the next step, the obtained solution is used as the known function, while the solution in the second direction is re-determined by another Kantorovich solution process. These iterations are repeated until the result converges to a desired degree. In the present work one-term approximation was used in the Kantorovich method. This expansion enables to obtain only approximate results for the natural frequencies, and for the vibration mode shapes. The exact modes will have curved nodal lines, and the single-term expansion will result in straight nodal lines that are parallel to the plate edges. The convergence to approximate values of frequency is very rapid.

In the solution in one direction, the exact element method for the vibration analysis of members with variable cross-sections is used [19]. This approach provides for the derivation of the exact dynamic stiffness matrix. The natural frequency is found as a value that leads to the singularity of the stiffness matrix. Free vibrations of rectangular thick plates are analyzed by varying the plate-aspect ratios, and the thickness-width and taper ratios. Two types of thickness variations are considered, namely linear and parabolic, and various combinations of boundary conditions. The results obtained by both shear deformation theories (FOPT and HOPT) are compared with those from the classical plate theory (CPT) and with published results. Many new results are also given.

2. Analysis of shear deformable rectangular plates

Consider an isotropic rectangular plate of planform L_x by L_y with variable thickness $\bar{h}(x, y)$, which is separable function of the coordinates (x, y). The plate has arbitrary boundary conditions. The coordinate system is taken such that the $x-y$ plane coincides with the middle plane of the plate (see Fig. 1).

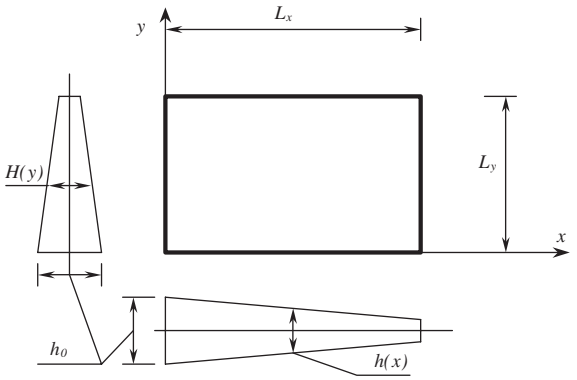

Fig. 1. Geometry and the coordinate system of rectangular plates with linear variation of thickness in both directions.

2.1. First-order shear deformation plate theory

According to the Reissner–Mindlin theory for harmonic motion, the displacement field is taken as

$$\bar{u}(x,y,z,t) = z\bar{\psi}_x(x,y,t) = z\psi_x(x,y)e^{i\omega t}, \tag{1a}$$

$$\bar{v}(x,y,z,t) = z\bar{\psi}_y(x,y,t) = z\psi_y(x,y)e^{i\omega t}, \tag{1b}$$

$$\bar{w}(x,y,z,t) = \bar{w}_0(x,y,t) = w_0(x,y)e^{i\omega t}, \tag{1c}$$

where $(\bar{u},\bar{v},\bar{w})$ are the displacement components along the (x, y, z) coordinate directions, respectively; $\bar{w}_0$ is the transverse deflection of a point on the middle plane, ψ_x and ψ_y denote the rotations around to the x and y axes, correspondingly and ω denotes the angular natural frequency. The displacement field of Eqs. (1a–c) results in the following expression for strain energy [9]:

$$U_{\max} = \frac{1}{2}\int\int_A \left\{ \begin{array}{l} \bar{D}\left(\begin{array}{c} \left(\frac{\partial\psi_x}{\partial x}\right)^2 + \left(\frac{\partial\psi_y}{\partial y}\right)^2 + 2\nu\frac{\partial\psi_x}{\partial x}\frac{\partial\psi_y}{\partial y} \\ +\frac{1}{2}(1-\nu)\left(\frac{\partial\psi_x}{\partial y}+\frac{\partial\psi_y}{\partial x}\right)^2 \end{array} \right) + \\ +k G\bar{h}\left(\psi_x + \frac{\partial w_0}{\partial x}\right)^2 + k G\bar{h}\left(\psi_y + \frac{\partial w_0}{\partial y}\right)^2 \end{array} \right\} \mathrm{d}x\mathrm{d}y, \tag{2}$$

where $\bar{D} = E\bar{h}^3/12/(1-\nu^2)$ is the bending rigidity of the plate, $G = E/2(1+\nu)$ is the shear modulus, E denotes Young's modulus of elasticity and ν is Poisson's ratio. The shear correction factor k is introduced to compensate for the discrepancy between the true parabolic distribution of transverse shear stresses and the constant state that resulted from the kinematic assumptions of this theory. For a comprehensive discussion on the value of the shear correction factor see Refs. [1,2].

For free vibration, the maximum kinetic energy can be expressed in terms of the general displacements, Eq. (1a–c), in the following form [9]:

$$T_{\max} = \frac{\omega^2\rho}{2}\iint_A \left[\bar{h}w_0^2 + \frac{\bar{h}^3}{12}\left(\psi_x^2 + \psi_y^2\right)\right] \mathrm{d}x\mathrm{d}y, \tag{3}$$

where ρ is the mass density of the plate's material.

The full energy functional Π can be written in terms of strain energy of bending and the kinetic energy of vibration as follow

$$\Pi = U_{\max} - T_{\max}. \tag{4}$$

According to the Kantorovich method, the solution is assumed separable, and can be written as

$$w_0(x,y) = w(x)W(y), \tag{5a}$$

$$\psi_x(x,y) = f(x)F(y), \tag{5b}$$

$$w(x,y) = w(x)W(y), \tag{5c}$$

In the same manner, the thickness of the plate $\bar{h}(x, y)$ is separated as

$$\bar{h}(x, y) = h_0 h(x) H(y), \tag{6}$$

where h_0 is the thickness at the origin, $h(x)$ and $H(y)$ are the functions of variation of the thickness in the x and y directions respectively (See Fig. 1). Based on Eqn. (6), the flexural rigidity of the plate $\bar{D}(x, y)$ becomes

$$\bar{D}(x, y) = d_0 d(x) D(y), \tag{7}$$

where

$$d_0 = Eh_0^3/(12(1 - v^2)); \quad d(x) = [h(x)]^3; \quad D(y) = [H(y)]^3.$$

For the convenience of subsequent derivation the following symbolism is defined: the lower case letters are used for functions of the x direction only, and capital letters for functions in the y direction. Two new variables are introduced as well

$$a_0 = \frac{h_0^3}{12}; \quad g_0 = kGh_0. \tag{8}$$

Substitutions of Eqs. (5a–c), their derivatives and Eqs. (6, 7) into Eq. (4) yield

$$\begin{aligned}
\Pi = \frac{1}{2}\int_0^{L_x}\int_0^{L_y} \Bigg[& df_{,x}^2 \underbrace{d_0 D F^2}_{S_1} + d\phi^2 \underbrace{d_0 D \Phi_{,y}^2}_{S_2} + 2df_{,x}\phi \underbrace{v d_0 D F \Phi_{,y}}_{S_3} \\
& + df^2 \underbrace{\frac{1}{2}(1-v) d_0 D F_{,y}^2}_{S_4} + 2df\phi_{,x} \underbrace{\frac{1}{2}(1-v) d_0 D F_{,y}\Phi}_{S_5} + d\phi_{,x}^2 \underbrace{\frac{1}{2}(1-v) d_0 D \Phi^2}_{S_6} \\
& + hf^2 \underbrace{g_0 H F^2}_{S_7} + 2hfw_{,x} \underbrace{g_0 H F W}_{S_8} + hw_{,x}^2 \underbrace{g_0 H W^2}_{S_9} + h\phi^2 \underbrace{g_0 H \Phi^2}_{S_{10}} + 2h\phi w \underbrace{g_0 H \Phi W_{,y}}_{S_{11}} \\
& + hw^2 \underbrace{g_0 H W_{,y}^2}_{S_{12}} - df^2 \underbrace{\omega^2 \rho a_0 D F^2}_{S_{13}} - d\phi^2 \underbrace{\omega^2 \rho a_0 D \Phi^2}_{S_{14}} - hw^2 \underbrace{\omega^2 \rho h_0 H W^2}_{S_{15}} \Bigg] \mathrm{d}x\mathrm{d}y.
\end{aligned} \tag{9}$$

In order to obtain equations involving only one variable, for example x, functions in the y direction are assumed for the time being as known, and after integration over this direction the energy functional take the form

$$\Pi = \frac{1}{2}\int_0^{L_x} \begin{pmatrix} S_1 df_{,x}^2 + S_2 d\phi^2 + 2S_3 df_{,x}\phi + S_4 df^2 + 2S_5 df\phi_{,x} + S_6 d\phi_{,x}^2 \\ +S_7 hf^2 + 2S_8 hf w_{,x} + S_9 hw_{,x}^2 + S_{10} h\phi^2 + 2S_{11} h\phi\, w + S_{12} h\, w^2 \\ -S_{13} df^2 - S_{14} d\phi^2 - S_{15} hw^2 \end{pmatrix} \mathrm{d}x, \tag{10}$$

where the coefficients S_1 through S_{15} are defined as

$$
\begin{aligned}
S_1 &= \int_0^{L_y} d_0 D F^2 \mathrm{d}y, \quad S_2 = \int_0^{L_y} \mathrm{d}_0 D \Phi_{,y}^2 \mathrm{d}y, \\
S_3 &= \int_0^{L_y} v d_0 D F \Phi_{,y} \mathrm{d}y, \quad S_4 = \int_0^{L_y} \frac{1}{2}(1-v) d_0 D F_{,y}^2 \mathrm{d}y, \\
S_5 &= \int_0^{L_y} \frac{1}{2}(1-v) d_0 D F_{,y} \Phi \, \mathrm{d}y, \quad S_6 = \int_0^{L_y} \frac{1}{2}(1-v) d_0 D \Phi^2 \mathrm{d}y, \\
S_7 &= \int_0^{L_y} g_0 H F^2 \mathrm{d}y \quad S_8 = \int_0^{L_y} g_0 H \, F W dy, \\
S_9 &= \int_0^{L_y} g_0 H W^2 \mathrm{d}y, \quad S_{10} = \int_0^{L_y} g_0 H \Phi^2 \mathrm{d}y, \\
S_{11} &= \int_0^{L_y} g_0 H \Phi W_{,y} \mathrm{d}y, \quad S_{12} = \int_0^{L_y} g_0 H W_{,y}^2 \mathrm{d}y, \\
S_{13} &= \int_0^{L_y} \omega^2 \rho a_0 D \, F^2 \mathrm{d}y, \quad S_{14} = \int_0^{L_y} \omega^2 \rho a_0 A \Phi^2, \\
S_{15} &= \int_0^{L_y} \omega^2 \rho \, h_0 H W^2.
\end{aligned} \tag{11}
$$

The evaluation of these constants will be performed after the assumption of the functions in the y direction is made (see Section 3).

According to the dynamic version of the principle of virtual displacement, i.e., Hamilton's principle the first variation of the functional should be equal to zero. Thus, variation of Eq. (10) and integration by parts yields

$$
\begin{aligned}
\delta \Pi = \int_0^{L_x} & \left(\begin{array}{l}
\left(\begin{array}{c} S_{11} h \phi + S_{12} h w - S_{15} h w - S_8 h_{,x} f - S_8 h f_{,x} + \\ - S_9 h_{,x} w_{,x} - S_9 h w_{,xx} \end{array} \right) \delta w \\
+ \left(\begin{array}{c} S_4 d f + S_5 d \phi_{,x} + S_7 h f + S_8 h w_{,x} - S_{13} d f + \\ - S_1 d_{,x} f_{,x} - S_1 d f_{,xx} - S_3 d_{,x} \phi - S_3 d \phi_{,x} \end{array} \right) \delta f \\
+ \left(\begin{array}{c} S_2 d \phi + S_3 d f_{,x} + + S_{10} h \phi + S_{11} h w - S_{14} d \phi + \\ - S_5 d_{,x} f - S_5 d f_{,x} - S_6 d_{,x} \phi_{,x} - S_6 d \phi_{,xx} \end{array} \right) \delta \phi
\end{array} \right) \mathrm{d}x \\
& + \left(S_8 h f + S_9 h w_{,x} \right) \delta w \big|_0^{L_x} \\
& + \left(S_1 d f_{,x} + S_3 d \phi \right) \delta f \big|_0^{L_x} \\
& + \left(S_5 d f + S_6 d \phi_{,x} \right) \delta \phi \big|_0^{L_x} = 0.
\end{aligned} \tag{12}
$$

Each term in the above equation has to be equal to zero. From the first integral, the system of differential equations is obtained:

$$\begin{aligned}\text{for } \delta w: \quad & -S_9 h w_{,xx} - S_9 h_{,x} w_{,x} + (S_{12} - S_{15}) h w \\ & - S_8 h f_{,x} - S_8 h_{,x} f + S_{11} h \phi = 0;\end{aligned} \tag{13a}$$

$$\begin{aligned}\text{for } \delta f: \quad & -S_1 d f_{,xx} - S_1 d_{,x} f_{,x} + S_4 d f + S_7 h f - S_{13} a f + S_8 h w_{,x} \\ & + (S_5 - S_3) d \phi_{,x} - S_3 d_{,x} \phi = 0;\end{aligned} \tag{13b}$$

$$\begin{aligned}\text{for } \delta \phi: \quad & -S_6 d \phi_{,xx} - S_6 d_{,x} \phi_{,x} + S_2 d \phi + S_{10} h \phi - S_{14} d \phi + S_{11} h w \\ & + (S_3 - S_5) d f_{,x} - S_5 d_{,x} f = 0.\end{aligned} \tag{13c}$$

The remaining expressions give the natural boundary conditions

$$\delta w: Q = \left(S_8 h f + S_9 h w_{,x}\right)\Big|_0^{L_x}, \tag{14a}$$

$$\delta f: M_b = \left(S_1 d f_{,x} + S_3 d \phi\right)\Big|_0^{L_x}, \tag{14b}$$

$$\delta \phi: M_t = \left(S_5 d f + S_6 d \phi_{,x}\right)\Big|_0^{L_x}, \tag{14c}$$

where Q is the shear force, M_b is the bending moment and M_t is the twisting moment on the corresponding edge of the plate.

The dimensionless coordinates $\xi = x/L_x$ and $\eta = y/L_y$ are used for the solution of the system of Eqs. (13a–c). The unknown displacements are assumed as infinite power series of the following form:

$$w(\xi) = \sum_{i=0}^{\infty} w_i \xi^i, \tag{15a}$$

$$f(\xi) = \sum_{i=0}^{\infty} f_i \xi^i, \tag{15b}$$

$$\phi(\xi) = \sum_{i=0}^{\infty} \phi_i \xi^i. \tag{15c}$$

Also the flexural rigidity and thickness parameters of the plate are taken in polynomial form as follows

$$d(\xi) = \sum_{j=0}^{n} d_j \xi^j, \tag{16a}$$

$$h(\xi) = \sum_{j=0}^{m} h_j \xi^j, \tag{16b}$$

where m, n are integers expressing the number of terms in each series. This description is very general, and many functions can be represented in this way to any desired accuracy.

All the polynomial coefficients w_i, f_i and ϕ_i of Eqs. (15a–c) can be found based on the first two terms of the each series [9,19]. Recurrence formulas for calculations of the w_{i+2}, f_{i+2} and ϕ_{i+2} are obtained by substituting the assumed polynomial functions of Eqs. (15a–c, 16a–b) and their

derivatives into the system of Eqs. (13a–c) (See Appendix A). The first two terms of each series should be found using the boundary condition [9,19]. Based on this solution technique, the exact shape functions for dynamic stiffness matrix assembling can be calculated. The degrees of freedom, for the FOPT formulation, are the lateral displacement and two rotations around the x and y axes at both ends of the strip element. The detail derivations of the stiffness matrix terms are given in Ref. [9].

2.2. Higher-order shear deformation plate theory

The displacement fields for the Third-order shear deformation plate theory of Reddy [1] are taken as

$$\bar{u}(x,y,z,t) = \left(z\psi_x - \frac{4z^3}{3h^2}\left(\psi_x + \frac{\partial w_0}{\partial x}\right)\right)e^{i\omega t}, \tag{17a}$$

$$\bar{v}(x,y,z,t) = \left(z\psi_y - \frac{4z^3}{3h^2}\left(\psi_y + \frac{\partial w_0}{\partial y}\right)\right)e^{i\omega t}, \tag{17b}$$

$$\bar{w}(x,y,z,t) = w_0 e^{i\omega t}. \tag{17c}$$

Based on the above displacement fields, the strain energy of the plate can be written as follows [9]

$$\begin{aligned} U = \frac{1}{2}\int_0^{L_y}\int_0^{L_x}\Bigg\{ & \bar{D}\Bigg[\frac{68}{105}\left(\frac{\partial\psi_x}{\partial x}\right)^2 + \frac{68}{105}\left(\frac{\partial\psi_y}{\partial y}\right)^2 + \frac{1}{21}\left(\frac{\partial^2 w}{\partial x^2}\right)^2 + \frac{1}{21}\left(\frac{\partial^2 w}{\partial y^2}\right)^2 \\ & - \frac{32}{105}\frac{\partial\psi_x}{\partial x}\frac{\partial^2 w}{\partial x^2} - \frac{32}{105}\frac{\partial\psi_y}{\partial y}\frac{\partial^2 w}{\partial y^2} + 2\nu\left(\frac{68}{105}\frac{\partial\psi_x}{\partial x}\frac{\partial\psi_y}{\partial y} + \frac{1}{21}\frac{\partial^2 w_0}{\partial y^2}\frac{\partial^2 w_0}{\partial x^2}\right. \\ & \left. - \frac{16}{105}\frac{\partial\psi_x}{\partial x}\frac{\partial^2 w_0}{\partial y^2} - \frac{16}{105}\frac{\partial\psi_y}{\partial y}\frac{\partial^2 w_0}{\partial x^2}\right) + \frac{(1-\nu)}{2}\left(\frac{68}{105}\left(\frac{\partial\psi_x}{\partial y}\right)^2 + \frac{68}{105}\left(\frac{\partial\psi_y}{\partial x}\right)^2\right. \\ & \left. + \frac{136}{105}\frac{\partial\psi_x}{\partial y}\frac{\partial\psi_y}{\partial x} + \frac{4}{21}\left(\frac{\partial^2 w_0}{\partial x\partial y}\right)^2 - \frac{64}{105}\frac{\partial^2 w_0}{\partial x\partial y}\frac{\partial\psi_x}{\partial y} - \frac{64}{105}\frac{\partial^2 w_0}{\partial x\partial y}\frac{\partial\psi_y}{\partial x}\right)\Bigg] \\ & + \frac{8}{15}G\bar{h}\left(\psi_x + \frac{\partial w}{\partial x}\right)^2 + \frac{8}{15}G\bar{h}\left(\psi_y + \frac{\partial w}{\partial y}\right)^2\Bigg\}\mathrm{d}x\mathrm{d}y. \end{aligned} \tag{18}$$

Utilization of the Kantorovich solution technique and integration over the y direction yields

$$U = \frac{1}{2}\int_0^{L_x}\left\{\begin{array}{c} S_1 df_{,x}^2 + S_2 d\phi^2 + S_3 dw_{,xx}^2 + S_4 dw^2 - 2S_5 df_{,x} w_{,xx} \\ +2S_6 d\phi w + 2S_7 df_{,x}\phi - 2S_8 df_{,x} w + 2S_9 d\phi w_{,xx} \\ +2S_{10} dw w_{,xx} + S_{11} df^2 + S_{12} d\phi_{,x}^2 + 2S_{13} df\phi_{,x} \\ +S_{14} dw_{,x}^2 - 2S_{15} dw_{,x} f - 2S_{16} dw_{,x}\phi_{,x} + S_{17} hf^2 \\ +2S_{18} hf w_{,x} + S_{19} hw_{,x}^2 + S_{20} h\phi^2 + 2S_{21} h\phi w + S_{22} hw^2 \end{array}\right\}\mathrm{d}x, \tag{19}$$

where the S-coefficients are defined as

$$S_1 = \int_0^{L_y} \frac{68}{105} d_0 D F^2 \, \mathrm{d}y, \quad S_2 = \int_0^{L_y} \frac{68}{105} d_0 D \Phi_{,y}^2 \, \mathrm{d}y,$$
$$S_3 = \int_0^{L_y} \frac{1}{21} d_0 D W^2 \, \mathrm{d}y, \quad S_4 = \int_0^{L_y} \frac{1}{21} d_0 D W_{,yy}^2 \, \mathrm{d}y,$$
$$S_5 = \int_0^{L_y} \frac{16}{105} d_0 D F W \, \mathrm{d}y, \quad S_6 = \int_0^{L_y} -\frac{16}{105} d_0 D \Phi_{,y} W_{,yy} \, \mathrm{d}y,$$
$$S_7 = \int_0^{L_y} \frac{68}{105} \nu d_0 D F \Phi_{,y} \, \mathrm{d}y, \quad S_8 = \int_0^{L_y} \frac{16}{105} \nu d_0 D F W_{,yy} \, \mathrm{d}y,$$
$$S_9 = \int_0^{L_y} -\frac{16}{105} \nu d_0 D \Phi_{,y} W \, \mathrm{d}y, \quad S_{10} = \int_0^{L_y} \frac{1}{21} \nu d_0 D W W_{,yy} \, \mathrm{d}y,$$
$$S_{11} = \int_0^{L_y} \frac{34}{105} (1-\nu) d_0 D F_{,y}^2 \, \mathrm{d}y, \quad S_{12} = \int_0^{L_y} \frac{34}{105} (1-\nu) d_0 D \Phi^2 \, dy,$$
$$S_{13} = \int_0^{L_y} \frac{34}{105} (1-\nu) d_0 D F_{,y} \Phi \, \mathrm{d}y, \quad S_{14} = \int_0^{L_y} \frac{2(1-\nu)}{21} d_0 D W_{,y}^2 \, \mathrm{d}y$$
$$S_{15} = \int_0^{L_y} \frac{16}{105} (1-\nu) d_0 D F_{,y} W \, \mathrm{d}y, \quad S_{16} = \int_0^{L_y} \frac{16}{105} (1-\nu) d_0 D \Phi W \, \mathrm{d}y,$$
$$S_{17} = \int_0^{L_y} \frac{8}{15} G h_0 H F^2 \, \mathrm{d}y, \quad S_{18} = \int_0^{L_y} \frac{8}{15} G h_0 H F W \, \mathrm{d}y,$$
$$S_{19} = \int_0^{L_y} \frac{8}{15} G h_0 H W^2 \, \mathrm{d}y, \quad S_{20} = \int_0^{L_y} \frac{8}{15} G h_0 H \Phi^2 \, \mathrm{d}y,$$
$$S_{21} = \int_0^{L_y} \frac{8}{15} G h_0 H \Phi W_{,y} \, \mathrm{d}y, \quad S_{22} = \int_0^{L_y} \frac{8}{15} G h_0 H W_{,y}^2 \, \mathrm{d}y. \tag{20}$$

The assumed free vibration is harmonic and based on the displacement field of Eqs. (17a–c), the expression of kinetic energy takes the following form [9]:

$$T = \omega^2 \frac{\rho}{2} \int \int_A \begin{bmatrix} \frac{17}{315} h^3 \psi_x^2 + \frac{17}{315} h^3 \psi_y^2 \\ + \frac{8}{315} h^3 \psi_x \frac{\partial w_0}{\partial x} + \frac{8}{315} h^3 \psi_y \frac{\partial w_0}{\partial y} \\ + h w^2 + \frac{h^3}{252} \left(\frac{\partial w_0}{\partial x}\right)^2 + \frac{h^3}{252} \left(\frac{\partial w_0}{\partial y}\right)^2 \end{bmatrix} \mathrm{d}x \mathrm{d}y. \tag{21}$$

Separation of the variables (Eqs. 5a–c) and integration over assumed direction, using the notation of Eqs. (7) and (8), yield

$$T = \frac{1}{2} \int_0^{L_x} \left\{ \begin{matrix} -S_{23} d f^2 - S_{24} d \phi^2 + 2 S_{25} d f w_{,x} - 2 S_{26} d \phi w \\ -S_{27} h w^2 + S_{28} d w_{,x}^2 - S_{29} d w^2 \end{matrix} \right\} \mathrm{d}x, \tag{22}$$

where S_{23} through S_{29} are

$$S_{23} = \int_0^{L_y} -\frac{17}{315}\omega^2\rho a_0 DF^2 \,\mathrm{d}y, \quad S_{24} = \int_0^{L_y} -\frac{17}{315}\omega^2\rho a_0 A\Phi^2 \,\mathrm{d}y,$$
$$S_{25} = \int_0^{L_y} \frac{4}{315}\omega^2\rho a_0 DFW \,\mathrm{d}y, \quad S_{26} = \int_0^{L_y} -\frac{4}{315}\omega^2\rho a_0 A\Phi W_{,y} \,\mathrm{d}y,$$
$$S_{27} = \int_0^{L_y} -\omega^2\rho h_0 HW^2 \,\mathrm{d}y, \quad S_{28} = \int_0^{L_y} \frac{1}{252}\omega^2\rho a_0 AW^2 \,\mathrm{d}y.$$
$$S_{29} = \int_0^{L_y} -\frac{1}{252}\omega^2\rho a_0 DW_{,y}^2 \,\mathrm{d}y, \tag{23}$$

According to Hamilton's principle the first variation of the functional should be equal to zero

$$\delta\Pi = \delta U - \delta T = 0. \tag{24}$$

After integrating the expressions of virtual energy by parts and collecting the coefficients of δw, δf and $\delta\phi$, the three equations of motion for the strip element are obtained in following form:

for δw:

$$\begin{pmatrix} S_3 dw_{,xxxx} + 2S_3 d_{,x} w_{,xxx} + S_3 d_{,xx} w_{,xx} + (2S_{10} - S_{14}) dw_{,xx} - S_{19} hw_{,xx} \\ +S_{28} dw_{,xx} + (2S_{10} - S_{14}) d_{,x} w_{,x} - S_{19} h_{,x} w_{,x} + S_{28} d_{,x} w_{,x} + S_{10} d_{,xx} w \\ +S_4 dw + (S_{22} + S_{27}) hw + S_{29} dw - S_5 df_{,xxx} - 2S_5 d_{,x} f_{,xx} - S_5 d_{,xx} f_{,x} \\ +(S_{15} - S_8) df_{,x} - S_{18} hf_{,x} + S_{25} df_{,x} + S_{15} d_{,x} f - S_{18} h_{,x} f + S_{25} d_{,x} f \\ +S_9 d\phi_{,xx} + S_{16} d\phi_{,xx} + (2S_9 + S_{16}) d_{,x}\phi_{,x} + S_9 d_{,xx}\phi + S_6 d\phi + S_{21} h\phi + S_{26} d\phi \end{pmatrix} = 0; \tag{25a}$$

for δf:

$$\begin{pmatrix} S_5 dw_{,xxx} + S_5 d_{,x} w_{,xx} + (S_8 - S_{15}) dw_{,x} + S_{18} hw_{,x} \\ -S_{25} dw_{,x} + S_8 d_{,x} w - S_1 df_{,xx} - S_1 d_{,x} f_{,x} + S_{11} df \\ +S_{17} hf + S_{23} df + (S_{13} - S_7) d\phi_{,x} - S_7 d_{,x}\phi \end{pmatrix} = 0; \tag{25b}$$

for $\delta\phi$:

$$\begin{pmatrix} (S_9 + S_{16}) dw_{,xx} + S_{16} d_{,x} w_{,x} + S_6 dw + S_{21} hw + S_{26} dw \\ (S_7 - S_{13}) df_{,x} - S_{13} d_{,x} f - S_{12} d\phi_{,xx} - S_{12} d_{,x}\phi_{,x} \\ +S_2 d\phi + S_{20} h\phi + S_{24} d\phi \end{pmatrix} = 0. \tag{25c}$$

The natural boundary conditions (forces and moments at the ends of strip elements) are obtained as

$$\delta w : Q = \begin{pmatrix} -S_3 dw_{,xxx} - S_3 d_{,x} w_{,xx} + (S_{14} - S_{10}) dw_{,x} + S_{19} hw_{,x} \\ -S_{28} dw_{,x} - S_{31} w_{,x} - S_{33} w - S_{10} d_{,x} w \\ +S_5 df_{,xx} + S_5 d_{,x} f_{,x} - S_{15} df + S_{18} hf - S_{25} df \\ -(S_9 + S_{16}) d\phi_{,x} - S_9 d_{,x}\phi \end{pmatrix} |_0^{L_x}, \tag{26a}$$

$$\delta w_{,x} : R = \left(S_3 dw_{,xx} - S_5 df_{,x} + S_9 d\phi + S_{10} dw\right)\Big|_0^{L_x}, \tag{26b}$$

$$\delta f : M_b = \left(S_1 df_{,x} - S_5 dw_{,xx} + S_7 d\phi - S_8 dw\right)\Big|_0^{L_x}, \tag{26c}$$

$$\delta \phi : M_t = \left(S_{12} d\phi_{,x} + S_{13} df - S_{16} dw_{,x}\right)\Big|_0^{L_x} \tag{26d}$$

Note that unlike the FOPT, an additional higher-order bending moment R appears in the HOPT approach.

The dimensionless variables ξ and η, and the assumption of polynomial variation of the all functions over the strip, Eqs. (15a–c) and (16a–b), are used again for the solution. The recurrence formulas for the polynomial terms, which are obtained by substituting the assumed functions into the Eqs. (26a–c) [9], are given in Appendix B. The rest of procedure is the same as in [9].

3. Numerical examples and discussion

In order to obtain a high precision solution for the free vibration problem of thick plates with polynomial variation of thickness, and simultaneously demonstrate the applicability and versatility of the present method, numerical calculations have been performed for a large number of plates with variable thickness for different taper ratios, length–width ratios, thickness–width ratios and various combinations of boundary conditions. The frequencies are expressed in terms of the dimensionless factor $\lambda = \omega L_y^2(\rho h_0/d_0)^{1/2}/\pi^2$. Nine dimensionless frequency values are given for each case based on the three plate theories (CPT, FOPT, HOPT). The mode shapes of vibration are defined by m and n, where these integers indicate the number of half-waves in the x and y directions, respectively. In all calculations, Poisson's ratio v is taken as 0.3. For the FOPT solutions the shear correction factor $k = 5/6$ is adopted [1,2]. The types of boundary conditions which are used are:

Simply Supported-S	for FOPT : $w = \phi = 0, M_b = 0,$
	for HOPT : $w = \phi = 0, M_b = R = 0;$
Simply Supported-S*	for FOPT : $w = 0, M_b = M_t = 0,$
	for HOPT : $w = 0, M_b = R = M_t = 0;$
Clamped - C	for FOPT : $w = f = \phi = 0,$
	for HOPT : $w = w_{,\xi} = f = \phi = 0;$
Free - F	for FOPT : $Q = M_b = M_t = 0,$
	for HOPT : $Q = M_b = R = M_t = 0.$

The plates are described by a symbolism defining the boundary conditions at their edges starting from $x = 0$ to $x = L_x$, $y = 0$, $y = L_y$ consequently. For example, CCFS denotes a plate with clamped edges at $x = 0$ and $x = L_x$, free at $y = 0$ and simply supported at $y = L_y$. Two types of the thickness variations are considered, namely linear and parabolic variations. The linear variation of thickness is shown in Fig. 1 and defined as

$$\bar{h}(x, y) = h_0 h(x) H(y) = h_0\left(1 - \beta_x \xi\right)\left(1 - \beta_y \eta\right), \tag{27}$$

where β_x and β_y are the taper ratios in the x and y directions respectively defined as $\beta_x = (h_0 - h(L_x))/h_0$ and $\beta_y = (h_0 - H(L_y))/h_0$.

Three forms of the parabolic variation of the thickness in the x direction are investigated, namely arched, concave, and symmetric concave variations (Fig. 2). The arched form is given by

$$\bar{h}(x,y) = h_0\left(1 - \delta\xi^2\right), \quad \delta = 1 - h_L/h_0. \tag{28a}$$

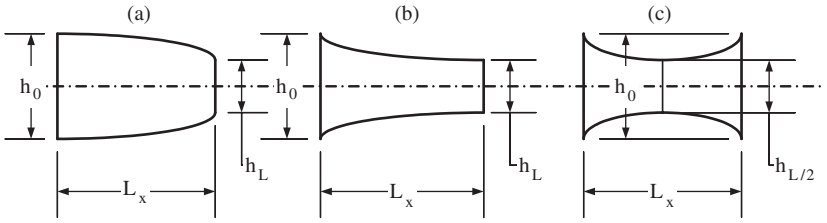

Fig. 2. Parabolic variations of the plate thickness: (a) arched form; (b) concave form; (c) symmetric concave form.

Table 1
Comparison of the frequency factors λ for x direction tapered Reissner–Mindlin square plates, ($v = 0.3$, $k = \pi^2/12$, $\beta_x = 0.5$)

Work	h_0/L_y	Mode							
		1,1	1,2	2,1	2,2	1,3	3,1	3,2	2,3
SSSS									
Present	0.1	1.4504	3.4743	3.5058	5.4838	6.5345	6.7038	8.5303	8.5921
Mizusawa [15]		1.4504	3.4743	3.5058	5.4840	6.5347	6.7039	8.5302	—
Present	0.2	1.3738	3.1096	3.1276	4.6613	5.4883	5.5657	6.8435	6.8725
Mizusawa [15]		1.3738	3.1096	3.1276	4.6613	5.4881	5.5656	6.8437	6.8726
Present	0.4	1.1664	2.3603	2.3637	3.2845	3.7942	3.8050	4.5043	4.5105
Mizusawa [15]		1.1665	2.3603	2.3637	3.2845	3.7942	3.8050	4.5043	4.5105

Work	h_0/L_y	Mode						
		1,1	1,2	2,1	1,3	2,2	2,3	3,1
SSFF								
Present	0.1	0.7201	1.2119	2.5569	2.6320	3.5362	4.9141	5.2300
Mikami and [12]		0.7226	1.2118	2.5561	2.6309	3.5362	—	—
Mizusawa [15]		0.7201	1.2119	2.5570	2.6320	3.5362	4.9142	—
Present	0.2	0.6999	1.1414	2.3663	2.3780	3.1050	4.1894	4.5840
Mikami and Yoshimura [12]		0.7000	1.1410	2.3661	2.3776	3.1054	—	—
Mizusawa [15]		0.6999	1.1414	2.3663	2.3780	3.1050	4.1894	4.5840
Present	0.4	0.6368	0.9668	1.9134	1.8534	2.2922	2.9752	3.3735
Mikami and Yoshimura [12]		0.6370	0.9666	1.8532	1.9135	2.2924	—	—
Mizusawa [15]		0.6368	0.9668	1.8534	1.9013	2.2922	2.9751	3.3735

The concave parabolic variation is expressed by

$$\bar{h}(x,y) = h_0\left(\delta\xi^2 - 2\delta\xi + 1\right), \quad \delta = 1 - h_L/h_0. \tag{28b}$$

The symmetric concave shape is given by

$$\bar{h}(x,y) = h_0\left(4\delta\xi^2 - 4\delta\xi + 1\right), \quad \delta = 1 - h_{0.5L}/h_0. \tag{28c}$$

The results obtained by the three theories are presented in table form for the different configurations of the rectangular plates. For each case the thickness-width ratio h/L_y are varied from 0.1 to 0.4. Note that ratios $h/L_y = 0.4$ does not really ascribe to a plate, but it is used for comparison and confirmation of the obtained results.

Table 2
Frequency factor λ for CCCC plates with linear thickness variation in the x direction

L_x/L_y	Theory	h_0/L_y	Mode								
			1,1	2,1	3,1	1,2	2,2	3,2	1,3	2,3	3,3
$\beta_x = 0.25$											
1	CPT	—	3.1767	6.4782	11.6375	6.4650	9.5610	14.5677	11.5703	14.5959	19.4425
	FOPT	0.1	2.9359	5.6690	9.5269	5.6634	8.0155	11.5315	9.5017	11.5459	14.6648
		0.2	2.4762	4.4051	6.8797	4.4053	5.9646	8.1386	6.8771	8.1431	10.0038
		0.3	2.0522	3.4468	5.1920	3.4483	4.5704	6.0848	5.1926	6.0865	7.3726
		0.4	1.7180	2.7842	4.1282	2.7855	3.6567	4.8110	4.1288	4.8116	5.7875
	HOPT	0.1	2.9401	5.6848	9.5699	5.6789	8.0466	11.5932	9.5434	11.6079	14.7608
		0.2	2.4955	4.4654	7.0156	4.4650	6.0651	8.3127	7.0112	8.3187	10.2488
		0.3	2.0894	3.5478	5.3939	3.5488	4.7268	6.3379	5.3933	6.3413	7.7148
		0.4	1.7713	2.9142	4.3699	2.9150	3.8486	5.1120	4.3696	5.1140	6.1863
1.5	CPT	—	2.3805	3.6844	5.8725	5.7909	7.0641	9.1165	10.8686	12.2946	14.2793
	FOPT	0.1	2.2374	3.3882	5.2347	5.1371	6.1415	7.7319	9.0369	9.9931	11.3724
		0.2	1.9385	2.8357	4.1795	4.0448	4.7456	5.8304	6.6004	7.1829	8.0699
		0.3	1.6404	2.3380	3.3354	3.1826	3.7119	4.5069	4.9999	5.4159	6.0548
		0.4	1.3935	1.9517	2.7316	2.5773	3.0040	3.6265	3.9824	4.3038	4.7980
	HOPT	0.1	2.2397	3.3932	5.2452	5.1494	6.1591	7.7575	9.0732	10.0391	11.4289
		0.2	1.9503	2.8575	4.2217	4.0959	4.8098	5.9151	6.7236	7.3244	8.2310
		0.3	1.6644	2.3792	3.4094	3.2711	3.8172	4.6407	5.1863	5.6237	6.2889
		0.4	1.4290	2.0100	2.8303	2.6920	3.1374	3.7935	4.2070	4.5552	5.0792
2	CPT	—	2.1598	2.8153	3.9554	5.5555	6.3038	7.3752	10.5530	11.5590	12.6485
	FOPT	0.1	2.0390	2.6267	3.6327	4.9549	5.5385	6.3948	8.8360	9.4841	10.2428
		0.2	1.7778	2.2507	3.0364	3.9236	4.3202	4.9328	6.4936	6.8522	7.3504
		0.3	1.5097	1.8911	2.5044	3.0929	3.3926	3.8605	4.9298	5.1743	5.5432
		0.4	1.2846	1.6006	2.0940	2.5053	2.7508	3.1283	3.9298	4.1162	4.4060
	HOPT	0.1	2.0409	2.6298	3.6377	4.9661	5.5530	6.4130	8.8695	9.5258	10.2903
		0.2	1.7881	2.2652	3.0583	3.9717	4.3768	4.9977	6.6110	6.9860	7.4930
		0.3	1.5312	1.9195	2.5455	3.1778	3.4869	3.9656	5.1098	5.3712	5.7506
		0.4	1.3167	1.6417	2.1519	2.6162	2.8708	3.2609	4.1472	4.3506	4.6564

In order to initiate the iterative procedure, initial functions should be assumed. According to the present formulations of the two higher-order shear deformation theories, the solution is a set of the dependent functions of the displacements. Therefore, in order to obtain correct relations between the assumed functions, so that they may satisfy any boundary conditions, the initial displacements are chosen as the lateral deflections and bending rotations of a Timoshenko beam for FOPT and high-order beams for HOPT [20]. Both polynomials are taken from the appropriate direction of the plate as a unit width strip. Although the beam shapes are not always congruent with the plate's displacement, the iteration convergence proves to be really fast. In the previous applications of the extended Kantorovich method [9,18] it has been shown that the initial assumed function is neither required to satisfy the essential boundary conditions nor the natural boundary conditions, and the quality of the assumption influences only the number of iterations. In the

Table 3
Frequency factor λ for CFFF plates with linear thickness variation in the x direction

L_x/L_y	Theory	h_0/L_y	Mode								
			1,1	2,1	3,1	1,2	2,2	3,2	1,3	2,3	3,3
$\beta_x = 0.5$											
1	CPT	—	0.3859	1.8485	4.7650	0.7563	2.4184	5.3746	1.9438	4.0317	7.2149
	FOPT	0.1	0.3828	1.7835	4.4122	0.7350	2.2981	4.9206	1.8669	3.7320	6.4338
		0.2	0.3737	1.6278	3.7222	0.6970	2.0598	4.1058	1.7335	3.2321	5.2280
		0.3	0.3610	1.4435	3.0866	0.6500	1.8029	3.3869	1.5831	2.7623	4.2552
		0.4	0.3458	1.2687	2.5955	0.6004	1.5752	2.8423	1.4380	2.3804	3.5464
	HOPT	0.1	0.3828	1.7842	4.4171	0.7352	2.2995	4.9268	1.8675	3.7353	6.4439
		0.2	0.3738	1.6324	3.7478	0.6979	2.0674	4.1356	1.7356	3.2463	5.2684
		0.3	0.3614	1.4553	3.1380	0.6524	1.8198	3.4433	1.5876	2.7905	4.3263
		0.4	0.3467	1.2889	2.6671	0.6048	1.6017	2.9186	1.4452	2.4223	3.6403
1.5	CPT	—	0.1713	0.8201	2.1130	0.4645	1.3244	2.6892	1.6458	2.7964	4.3733
	FOPT	0.1	0.1708	0.8063	2.0369	0.4519	1.2778	2.5535	1.5995	2.6447	4.0433
		0.2	0.1684	0.7703	1.8578	0.4323	1.1906	2.2856	1.5120	2.3811	3.4888
		0.3	0.1654	0.7210	1.6490	0.4083	1.0872	1.9997	1.4055	2.1054	2.9691
		0.4	0.1617	0.6665	1.4544	0.3824	0.9852	1.7482	1.2958	1.8601	2.5482
	HOPT	0.1	0.1708	0.8064	2.0376	0.4520	1.2783	2.5547	1.5995	2.6459	4.0465
		0.2	0.1684	0.7710	1.8623	0.4327	1.1927	2.2926	1.5127	2.3859	3.5018
		0.3	0.1654	0.7230	1.6604	0.4094	1.0923	2.0154	1.4069	2.1157	2.9955
		0.4	0.1618	0.6705	1.4735	0.3843	0.9940	1.7728	1.2982	1.8770	2.5888
2	CPT	—	0.0963	0.4606	1.1860	0.3353	0.9033	1.7220	1.5252	2.3179	3.2957
	FOPT	0.1	0.0961	0.4560	1.1607	0.3262	0.8758	1.6558	1.4899	2.2177	3.0957
		0.2	0.0952	0.4436	1.0968	0.3132	0.8283	1.5283	1.4191	2.0355	2.7496
		0.3	0.0941	0.4256	1.0129	0.2974	0.7707	1.3807	1.3292	1.8324	2.3988
		0.4	0.0927	0.4042	0.9248	0.2802	0.7109	1.2393	1.2638	1.6419	2.0959
	HOPT	0.1	0.0962	0.4560	1.1609	0.3263	0.8760	1.6564	1.4900	2.2183	3.0972
		0.2	0.0952	0.4438	1.0980	0.3134	0.8293	1.5310	1.4194	2.0377	2.7556
		0.3	0.0941	0.4261	1.0163	0.2980	0.7731	1.3871	1.3299	1.8372	2.4118
		0.4	0.0927	0.4053	0.9312	0.2813	0.7152	1.2500	1.2696	1.6501	2.1173

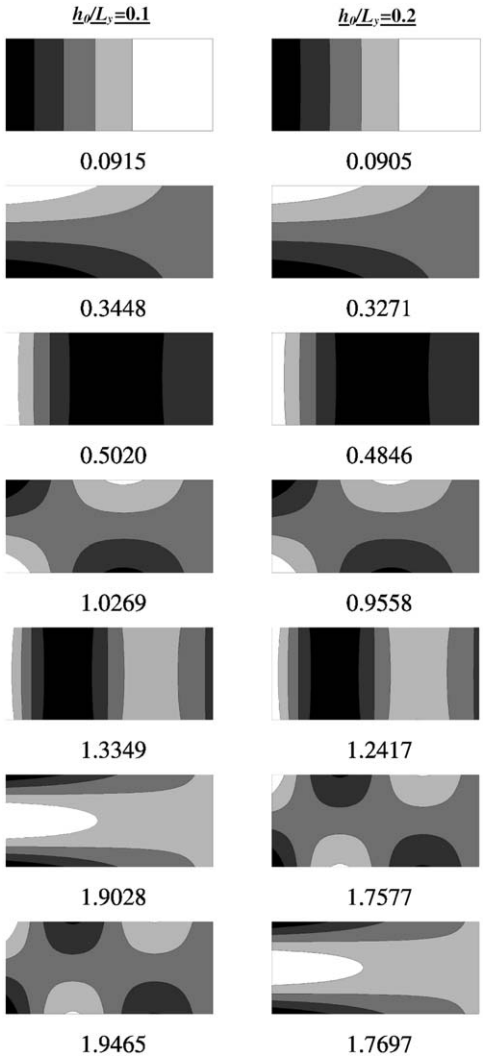

Fig. 3. Free vibration modes and normalized frequency factors for CFFF plates with linear thickness variation in the x direction: $L_x/L_y = 2.0$, $\beta_x = 0.25$: HOPT solution.

present work, the maximal tolerance for the relative error between the iteration steps is taken as 0.0001%. Unlike most of the other numerical methods, in which a better result is obtained by increasing the number of unknowns, the solution in the extended Kantorovich method is improved by continuous enhancement of the operator between successive iteration steps, without additional unknowns.

3.1. Plates with linear thickness variation in the x direction

It appears that there are no available results for rectangular plates with variable thickness computed based on any HOPT. Thus, the confirmation of the obtained results is made only with

Table 4
Frequency factor λ for CCCC square plates with linear thickness variation in the both directions

β_y	Theory	h_0/L_y	Mode								
			1,1	2,1	3,1	1,2	2,2	3,2	1,3	2,3	3,3
$\beta_x = 0.25$											
0.25	CPT	—	2.7667	5.6312	10.0754	5.6312	8.3356	12.7168	10.0754	12.7168	16.9537
	FOPT	0.1	2.6022	5.0733	8.6089	5.0733	7.2403	10.5229	8.6089	10.5229	13.4632
		0.2	2.2620	4.1002	6.4940	4.1002	5.6032	7.7258	6.4940	7.7258	9.5497
		0.3	1.9215	3.2895	5.0065	3.2895	4.3892	5.8875	5.0065	5.8875	7.1625
		0.4	1.6368	2.6965	4.0235	2.6965	3.5552	4.7022	4.0235	4.7022	5.6735
	HOPT	0.1	2.6048	5.0832	8.6359	5.0832	7.2606	10.5643	8.6359	10.5643	13.5291
		0.2	2.2749	4.1421	6.5921	4.1421	5.6763	7.8568	6.5921	7.8568	9.7365
		0.3	1.9479	3.3650	5.1574	3.3650	4.5104	6.0855	5.1632	6.0887	7.4302
		0.4	1.6765	2.7986	4.2192	2.7986	3.7105	4.9490	4.2192	4.9490	6.0012
0.5	CPT	—	2.3209	4.6823	8.2375	4.7261	7.0243	10.7602	8.4456	10.6858	14.3012
	FOPT	0.1	2.2208	4.3495	7.3887	4.3771	6.3217	9.3160	7.5108	9.2594	11.9744
		0.2	1.9951	3.6870	5.9211	3.6943	5.1208	7.1690	5.9556	7.1420	8.9131
		0.3	1.7458	3.0609	4.7226	3.0587	4.1284	5.6032	4.7272	5.5906	6.8489
		0.4	1.5210	2.5639	3.8633	2.5588	3.4021	4.5387	3.8614	4.5325	5.4969
	HOPT	0.1	2.2222	4.3545	7.4020	4.3826	6.3334	9.3408	7.5265	9.2842	12.0152
		0.2	2.0026	3.7119	5.9804	3.7208	5.1695	7.2616	6.0212	7.2324	9.0474
		0.3	1.7645	3.1060	4.8310	3.1110	4.2169	5.7586	4.8412	5.7407	7.0627
		0.4	1.5477	2.6374	4.0091	2.6339	3.5228	4.7383	4.0109	4.7264	5.7617
$\beta_x = 0.5$											
0.5	CPT	—	1.9473	3.9309	6.9087	3.9309	5.9193	9.0421	6.9087	9.0421	12.0635
	FOPT	0.1	1.8870	3.7253	6.3773	3.7253	5.4755	8.1202	6.3773	8.1202	10.5425
		0.2	1.7410	3.2764	5.3441	3.2764	4.6231	6.5491	5.3441	6.5491	8.2249
		0.3	1.5654	2.8060	4.3987	2.8060	3.8389	5.2674	4.3987	5.2674	6.4883
		0.4	1.3947	2.4028	3.6690	2.4028	3.2241	4.3392	3.6690	4.3392	5.2862
	HOPT	0.1	1.8876	3.7292	6.3851	3.7281	5.4820	8.1324	6.3845	8.1352	10.5669
		0.2	1.7453	3.2906	5.3936	3.2913	4.6543	6.6099	5.3802	6.6100	8.3036
		0.3	1.5755	2.8391	4.4729	2.8390	3.9002	5.3784	4.4734	5.3784	6.6475
		0.4	1.4119	2.4543	3.7759	2.4543	3.3138	4.4913	3.7759	4.4913	5.4973

existing FOPT solutions. Table 1 shows a comparison study of the natural frequency factors λ for two types of rectangular plates. As can be seen, similar or more precise results are achieved for every case.

The natural frequency factors λ for CCCC and CFFF plates tapered in the x-direction calculated by using the three theories are given in Tables 2 and 3. The frequencies decrease with an increase of the thickness-width ratio (h/L_y) for constant values of L_x/L_y. It is seen that this effect is more pronounced for higher modes. Such behavior is due to the influence of rotary inertia and shear deformations. Also, the discrepancy between the CPT results and the higher theories (HOPT, FOPT) becomes more significant because the CPT does not take into account the additional flexibility due to the shear stresses.

The comparison of the HOPT and FOPT results for the tapered SSSS square plate shows the difference between the results of these theories is very small in the cases of low thickness–width ratios, and exceeds 1% only for relatively thick plates ($h/L_y = 0.3, 0.4$) for the higher modes (two and more half waves). Also the influence of the thickness variation becomes smaller as the aspect ratio L_x/L_y increases. This effect ascribes to more flexibility of the longer plates.

The first seven modes for rectangular CFFF plate with linear variation of the thickness are presented in Fig. 3. It is seen that the increase in the thickness–width ratio causes not only the decrease of the values of the natural frequency factor, but also change the order of mode shapes (the 6th and 7th mode interchange).

3.2. Plates with linear thickness variation in both directions

The dimensionless factor of natural frequencies for CCCC and CFCF plates with linear variation thickness in the both directions are given in Tables 4 and 5. The first six modes for free vibration of the CFCF plate tapered in both directions are shown in Fig. 4. Although for this case the assumed separation, Eqs. (5a–c), provides only for approximate solution, the obtained shapes are true in principle.

Table 5
Frequency factor λ for CFCF square plates with linear thickness variation in the both directions

β_y	Theory	h_0/L_y	Mode								
			1,1	2,1	3,1	1,2	2,2	3,2	1,3	2,3	3,3
$\beta_x = 0.25$											
0.25	CPT	—	0.5787	1.9491	4.7245	1.9491	3.6621	6.6644	4.7245	6.6644	9.7979
	FOPT	0.1	0.5683	1.8698	4.3850	1.8698	3.3970	5.9657	4.3850	5.9657	8.4416
		0.2	0.5476	1.7033	3.7335	1.7033	2.9287	4.8490	3.7335	4.8490	6.5565
		0.3	0.5206	1.5116	3.1186	1.5116	2.4825	3.9319	3.1186	3.9319	5.1739
		0.4	0.4909	1.3308	2.6312	1.3308	2.1192	3.2594	2.6312	3.2594	4.2207
	HOPT	0.1	0.5685	1.8707	4.3889	1.8707	3.4003	5.9760	4.3889	5.9760	8.4640
		0.2	0.5481	1.7079	3.7524	1.7079	2.9442	4.8873	3.7524	4.8873	6.6237
		0.3	0.5218	1.5223	3.1589	1.5224	2.5132	4.0007	3.1589	4.0007	5.2861
		0.4	0.4930	1.3487	2.6888	1.3487	2.1641	3.3528	2.6888	3.3528	4.3682
0.5	CPT	—	0.5204	1.5659	3.6115	1.7129	3.0779	5.5512	4.0509	5.6196	8.2003
	FOPT	0.1	0.5144	1.5225	3.4491	1.6634	2.9172	5.1270	3.8322	5.1794	7.3421
		0.2	0.5012	1.4307	3.1064	1.5499	2.6046	4.3596	3.3716	4.3852	5.9722
		0.3	0.4830	1.3155	2.7260	1.4087	2.2748	3.6484	2.8937	3.6605	4.8501
		0.4	0.4617	1.1962	2.3817	1.2667	1.9844	3.0859	2.4891	3.0936	4.0271
	HOPT	0.1	0.5144	1.5229	3.4505	1.6639	2.9191	5.1320	3.8347	5.1853	7.3535
		0.2	0.5015	1.4328	3.1143	1.5529	2.6142	4.3831	3.3857	4.4117	6.0179
		0.3	0.4837	1.3206	2.7469	1.4163	2.2953	3.6953	2.9250	3.7116	4.9315
		0.4	0.4630	1.2054	2.4128	1.2800	2.0162	3.1535	2.5366	3.1654	4.1372

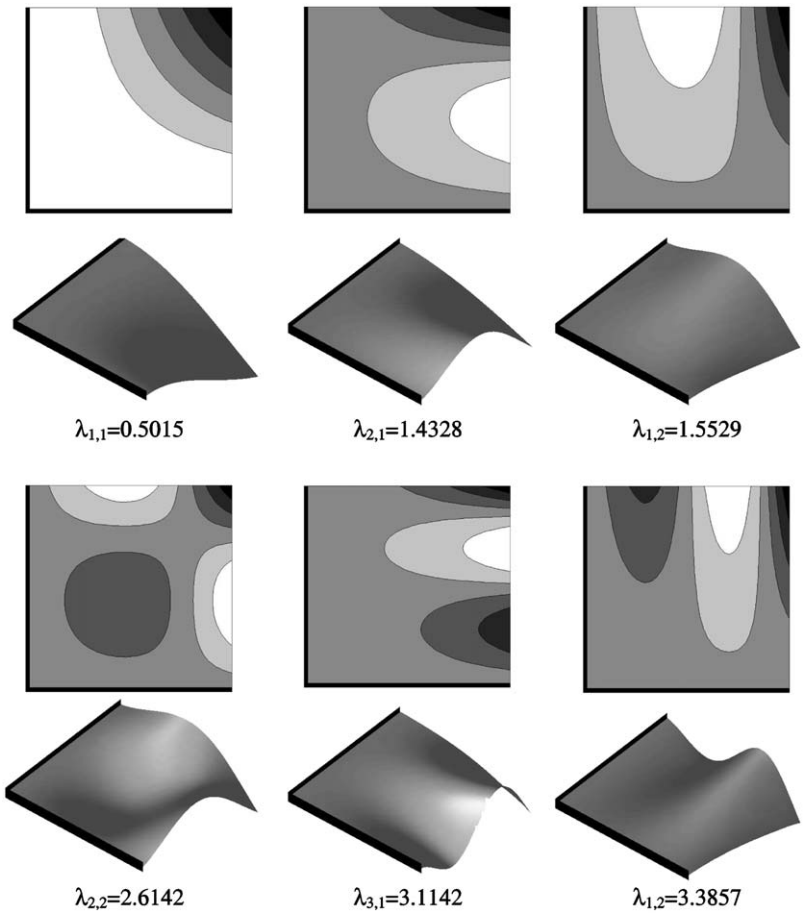

Fig. 4. Free vibration modes for CFCF square plate with linear thickness variation in both directions: $h_0/L_y = 0.2$, $\beta_x = 0.25$, $\beta_y = 0.5$, $v = 0.3$: HOPT solution.

Table 6
Comparison of the frequency factors λ for Reissner-Mindlin S*S*S*S* square plates with parabolic thickness variation in the x direction, (arched form, $\delta = 0.5$, $v = 0.3$,$k = \pi^2/12$)

h_0/L_y	Work	Mode							
		1 (1,1)	2 (2,1)	3 (1,2)	4 (2,2)	5 (1,3)	6 (3,1)	7 (3,2)	8 (2,3)
0.1	Present	1.5568	3.7959	3.8085	5.8475	7.2049	7.2655	9.0839	9.1839
	Al-Kaabi and Aksu [14]	1.5825	3.8732	3.8864	5.8834	7.4975	7.5683	9.1543	9.2762
0.2	Present	1.4279	3.2864	3.3032	4.7969	5.8422	5.8488	7.0432	7.0825
	Al-Kaabi and Aksu [14]	1.4526	3.3301	3.3452	4.8023	5.8752	5.8790	6.9424	6.9761

Table 7
Frequency factor λ for CCCC square plates with parabolic thickness variation in the x directions, (arched form)

δ	Theory	h_0/L_y	Mode								
			1,1	2,1	3,1	1,2	2,2	3,2	1,3	2,3	3,3
0.25	CPT	—	3.3157	6.7387	12.1298	6.8267	10.0079	15.2278	12.2594	15.3302	20.3699
	FOPT	0.1	3.0415	5.8365	9.7926	5.8986	8.2714	11.8566	9.8721	11.8998	15.0623
		0.2	2.5344	4.4779	6.9824	4.5100	6.0684	8.2589	7.0162	8.2702	10.1398
		0.3	2.0813	3.4768	5.2382	3.4945	4.6162	6.1380	5.2541	6.1418	7.4313
		0.4	1.7319	2.7952	4.1521	2.8067	3.6791	4.8374	4.1610	4.8390	5.8171
	HOPT	0.1	3.0465	5.8544	9.8405	5.9174	8.3072	11.9257	9.9223	11.9714	15.1703
		0.2	2.5565	4.5438	7.1279	4.5791	6.1795	8.4472	7.1695	8.4646	10.4066
		0.3	2.1230	3.5851	5.4512	3.6076	4.7855	6.4082	5.4773	6.4182	7.7980
		0.4	1.7906	2.9327	4.4043	2.9493	3.8835	5.1560	4.4240	5.1638	6.2286
0.5	CPT	—	2.9428	5.9543	10.7304	6.0915	8.9525	13.5535	10.7897	13.8529	18.2497
	FOPT	0.1	2.7420	5.2909	8.9859	5.4058	7.6223	10.9760	9.0766	11.1258	14.0809
		0.2	2.3434	4.1952	6.6405	4.2697	5.7661	7.9029	6.7123	7.9491	9.7694
		0.3	1.9623	3.3237	5.0699	3.3712	4.4605	5.9663	5.1128	5.9835	7.2572
		0.4	1.6545	2.7036	4.0551	2.7360	3.5884	4.7417	4.0810	4.7494	5.7207
	HOPT	0.1	2.7454	5.3031	9.0192	5.4186	7.6483	11.0260	9.1099	11.1809	14.1628
		0.2	2.3595	4.2446	6.7523	4.3229	5.8551	8.0531	6.8323	8.1146	9.9924
		0.3	1.9944	3.4098	5.2422	3.4649	4.6040	6.1933	5.3019	6.2284	7.5768
		0.4	1.7018	2.8176	4.2663	2.8584	3.7656	5.0132	4.3107	5.0368	6.0886

Table 8
Frequency factor λ for CCCC square plates with parabolic thickness variation in the x directions, (concave form)

δ	Theory	h_0/L_y	Mode								
			1,1	2,1	3,1	1,2	2,2	3,2	1,3	2,3	3,3
0.25	CPT	—	3.0380	6.2144	11.1380	6.1022	9.1095	13.8996	10.8766	13.8533	18.5053
	FOPT	0.1	2.8280	5.4937	9.2460	5.4175	7.7458	11.1863	9.1072	11.1680	14.2399
		0.2	2.4144	4.3255	6.7669	4.2899	5.8505	8.0060	6.7211	8.0022	9.8532
		0.3	2.0202	3.4123	5.1402	3.3954	4.5188	6.0249	5.1225	6.0241	7.3063
		0.4	1.7023	2.7701	4.1009	2.7605	3.6310	4.7804	4.0918	4.7799	5.7535
	HOPT	0.1	2.8316	5.5076	9.2843	5.4302	7.7727	11.2411	9.1412	11.2211	14.3245
		0.2	2.4311	4.3801	6.8932	4.3408	5.9407	8.1662	6.8369	8.1594	10.0771
		0.3	2.0533	3.5060	5.3309	3.4838	4.6624	6.2612	5.3013	6.2574	7.6241
		0.4	1.7503	2.8926	4.3318	2.8768	3.8102	5.0641	4.3105	5.0603	6.1271
0.5	CPT	—	2.3878	4.9025	8.7425	4.6537	7.1385	10.8896	8.1054	10.8098	14.5002
	FOPT	0.1	2.2835	4.5231	7.7170	4.3327	6.4168	9.3996	7.2995	9.3726	12.1072
		0.2	2.0494	3.7933	6.0592	3.6893	5.1880	7.2173	5.8872	7.2188	8.9821
		0.3	1.7915	3.1256	4.7835	3.0742	4.1753	5.6344	4.7155	5.6393	6.8881
		0.4	1.5591	2.6074	3.8976	2.5811	3.4362	4.5618	3.8663	4.5648	5.5225
	HOPT	0.1	2.2850	4.5294	7.7358	4.3375	6.4291	9.4270	7.3118	9.3971	12.1505
		0.2	2.0573	3.8233	6.1356	3.7129	5.2391	7.3159	5.9421	7.3121	9.1247
		0.3	1.8090	3.1841	4.9126	3.1223	4.2681	5.7962	4.8176	5.7978	7.1134
		0.4	1.5870	2.6905	4.0637	2.6519	3.5627	4.7677	4.0054	4.7688	5.7981

Table 9
Frequency factor λ for CCCC square plates with parabolic thickness variation in the x directions, (symmetric concave form)

δ	Theory	h_0/L_y	Mode								
			1,1	2,1	3,1	1,2	2,2	3,2	1,3	2,3	3,3
0.25	CPT	—	3.0944	6.3631	11.3249	5.9777	9.1365	14.0013	10.5448	13.7220	18.4921
	FOPT	0.1	2.8829	5.6132	9.3636	5.3408	7.7823	11.2528	8.9202	11.1268	14.2551
		0.2	2.4653	4.4062	6.8235	4.2703	5.8885	8.0423	6.6586	8.0103	9.8723
		0.3	2.0651	3.4700	5.1736	3.4013	4.5503	6.0484	5.1044	6.0394	7.3215
		0.4	1.7411	2.8154	4.1253	2.7756	3.6568	4.7988	4.0891	4.7951	5.7664
	HOPT	0.1	2.8866	5.6283	9.4064	5.3523	7.8094	11.3113	8.9504	11.1778	14.3415
		0.2	2.4822	4.4655	6.9629	4.3169	5.9799	8.2121	6.7636	8.1631	10.1006
		0.3	2.0985	3.5710	5.3816	3.4834	4.6961	6.2958	5.2695	6.2680	7.6439
		0.4	1.7898	2.9467	4.3749	2.8849	3.8395	5.0950	4.2935	5.0721	6.1474
0.5	CPT	—	2.5494	5.2154	9.1261	4.4997	7.2047	11.1009	7.6484	10.5409	14.4563
	FOPT	0.1	2.4367	4.7909	7.9973	4.2182	6.4917	9.5571	6.9687	9.2326	12.1207
		0.2	2.1852	3.9874	6.2143	3.6437	5.2693	7.3133	5.7265	7.2047	9.0165
		0.3	1.9087	3.2658	4.8745	3.0746	4.2482	5.6962	4.6488	5.6635	6.9251
		0.4	1.6600	2.7142	3.9593	2.6046	3.4975	4.6065	3.8434	4.5960	5.5529
	HOPT	0.1	2.4384	4.7987	8.0212	4.2222	6.5044	9.5888	6.9782	9.2545	12.1653
		0.2	2.1938	4.0240	6.3099	3.6633	5.3216	7.4261	5.7704	7.2886	9.1713
		0.3	1.9279	3.3361	5.0336	3.1151	4.3430	5.8780	4.7324	5.8079	7.1552
		0.4	1.6903	2.8126	4.1603	2.6653	3.6265	4.8340	3.9600	4.7850	5.8362

3.3. *Plates with parabolic thickness variation in the x-direction*

For confirmation, the available results from Ref. [14] are compared in Table 6 with those from the current study. It is seen that there is only a few percent difference between the results. This is because the results predicted by the energy-based finite difference solution technique [14] are generally higher than the expected value. The dimensionless values of natural frequencies for the three types of parabolic variation of thickness are given in Tables 7–9 for CCCC boundary conditions.

4. Conclusions

The free vibrations of rectangular thick plates with variable thickness and different boundary conditions have been investigated by using the extended Kantorovich method. This approach is combined with the exact element method for the vibration analysis of members with variable cross-section. Two shear deformation theories, in which the effects of both transverse shear stresses and rotary inertia are accounted for, have been applied to the analysis. The number of numerical examples demonstrates the applicability and versatility of the present method.

The advantages of the proposed method are:

- Any polynomial variation of the thickness throughout the plate can be considered.
- The shape functions are exact solutions for the system of the differential equations of motion and they are derived automatically. As a result, the solution for the free vibration problems is accurate (depending only on the accuracy of the numerical calculations), as the only approximation is assuming a one-term separable solution.
- The exact solution is guaranteed when at least two edges of constant thickness direction of the plate are simply supported and the problem is separable (Levy case). For other cases, it has been found that the proposed separation of variables, Eqs. (5a–c), leads to accurate natural frequency values and good approximation for the free vibration modes.

Acknowledgements

The support for this research to the first author by the Technion-Israel Institute of Technology is gratefully acknowledged. The authors thank the reviewers for their most important comments that improved the quality of the paper.

Appendix A. Recurrence formulas for FOPT solution

For $i = 0 \ldots \infty$:

$$w_{i+2} = \frac{1}{S_9 h_0 (i+1)(i+2)} \left[-S_9 \sum_{j=1}^{i} h_j (i-j+1)(i-j+2) w_{i-j+2} \right.$$
$$- S_9 \sum_{j=0}^{i} (j+1) h_{j+1} (i-j+1) w_{i-j+1} - S_8 L_x \sum_{j=0}^{i} (j+1) h_{j+1} f_{i-j}$$
$$\left. + (S_{12} - S_{15}) L_x^2 \sum_{j=0}^{i} h_j w_{i-j} - S_8 L_x \sum_{j=0}^{i} h_j (i-j+1) f_{i-j+1} + S_{11} L_x^2 \sum_{j=0}^{i} h_j \phi_{i-j} \right],$$

$$f_{i+2} = \frac{1}{S_1 d_0 (i+1)(i+2)} \left[-S_1 \sum_{j=1}^{i} d_j (i-j+1)(i-j+2) f_{i-j+2} \right.$$
$$- S_1 \sum_{j=0}^{i} (j+1) d_{j+1} (i-j+1) f_{i-j+1} - S_3 L_x \sum_{j=0}^{i} (j+1) d_{j+1} \phi_{i-j}$$
$$+ S_4 L_x^2 \sum_{j=0}^{i} d_j f_{i-j} + S_7 L_x^2 \sum_{j=0}^{i} h_j f_{i-j} - S_{13} L_x^2 \sum_{j=0}^{i} d_j f_{i-j}$$
$$\left. + S_8 L_x \sum_{j=0}^{i} h_j (i-j+1) w_{i-j+1} + (S_5 - S_3) L_x \sum_{j=0}^{i} d_j (i-j+1) \phi_{i-j+1} \right],$$

$$\phi_{i+2} = \frac{1}{S_6 d_0 (i+1)(i+2)} \Bigg[-S_6 \sum_{j=1}^{i} d_j (i-j+1)(i-j+2)\phi_{i-j+2} - S_6 \sum_{j=0}^{i} (j+1) d_{j+1} (i-j+1)\phi_{i-j+1} - S_5 L_x \sum_{j=0}^{i} (j+1) d_{j+1} f_{i-j} + S_2 L_x^2 \sum_{j=0}^{i} d_j \phi_{i-j} + S_{10} L_x^2 \sum_{j=0}^{i} h_j \phi_{i-j} - S_{14} L_x^2 \sum_{j=0}^{i} d_j \phi_{i-j} + S_{11} L_x^2 \sum_{j=0}^{i} h_j w_{i-j} + (S_3 - S_5) L_x \sum_{j=0}^{i} d_j (i-j+1) f_{i-j+1} \Bigg].$$

Appendix B. Recurrence formulas for HOPT solution

In contrast with the FOPT analysis, when unknown polynomial terms could be found one after another, in the current HOPT formulation the following algorithm should be used to calculate them.

Firstly, the f_2 term is calculated for $i = 0$ from the following expression:

$$f_2 = \frac{1}{2 S_1 L d_0} \begin{pmatrix} 6 S_5 d_0 w_3 + (S_8 - S_{15}) L_x^2 d_0 w_1 + S_{18} L_x^2 h_0 w_1 - S_{25} L_x^2 d_0 w_1 \\ + S_{11} L_x^2 d_0 f_0 + S_{17} L_x^2 h_0 f_0 + S_{23} L_x^3 d_0 f_0 + (S_{13} - S_7) L_x^2 d_0 \phi_1 \\ + 2 S_5 d_1 w_2 - S_1 L_x d_1 f_1 + S_8 L_x^2 d_1 w_0 - S_7 L_x^2 d_1 \phi_0 \end{pmatrix}.$$

Then for $i = 0 \ldots \infty$, the ϕ_{i+2} terms are determinated by

$$\phi_{i+2} = \frac{1}{S_{12} d_0 (i+2)!} \Bigg[-S_{12} \sum_{k=1}^{i} d_k \phi_{i-k+2} (i-k+2)! - S_{13} L_x \sum_{k=0}^{i} (k+1) d_{k+1} f_{i-k} + S_{16} \sum_{k=0}^{i} (k+1) d_{k+1} w_{i-k+1} (i-k+1) - S_{12} \sum_{k=0}^{i} (k+1) d_{k+1} \phi_{i-k+1} (i-k+1) + (S_9 + S_{16}) \sum_{k=0}^{i} d_k w_{i-k+2} (i-k+2)! + S_6 L_x^2 \sum_{k=0}^{i} d_k w_{i-k} + S_{21} L_x^2 \sum_{k=0}^{i} h_k w_{i-k} + S_{26} L_x^2 \sum_{k=0}^{i} a_k w_{i-k} + (S_7 - S_{13}) L_x \sum_{k=0}^{i} d_k f_{i-k+1} (i-k+1) + S_2 L_x^2 \sum_{k=0}^{i} d_k \phi_{i-k} + S_{20} L_x^2 \sum_{k=0}^{i} h_k \phi_{i-k} + S_{24} L_x^2 \sum_{k=0}^{i} a_k \phi_{i-k} \Bigg].$$

Now the terms w_{i+4} and f_{i+3} can be found from the system of two equations:

$$A_{1,1}^{(i)} w_{i+4} + A_{1,2}^{(i)} f_{i+3} = B_1^{(i)},$$
$$A_{2,1}^{(i+1)} w_{i+4} + A_{2,2}^{(i+1)} f_{i+3} = B_2^{(i)},$$

where the terms A, B are defined by the following expression:

$$A_{1,1}^{(i)} = -S_3 d_0 (i+4)(i+3)(i+2)(i+1),$$
$$A_{1,2}^{(i)} = S_5 L_x d_0 (i+3)(i+2)(i+1),$$
$$A_{2,1}^{(i)} = -S_5 d_0 (i+3)(i+2)(i+1),$$
$$A_{2,2}^{(i)} = S_1 L_x d_0 (i+2)(i+1),$$

$$\begin{aligned}
B_1^{(i)} = {} & S_3 \sum_{k=1}^{i} d_k w_{i-k+4} (i-k+4)! - S_5 L_x \sum_{k=1}^{i} d_k f_{i-k+3} (i-k+3)! \\
& + S_3 \sum_{k=0}^{i} (k+2)! d_{k+2} w_{i-k+2} (i-k+2)! + S_9 L_x^2 \sum_{k=0}^{i} (k+2)! d_{k+2} \phi_{i-k} \\
& - S_5 L_x \sum_{k=0}^{i} (k+2)! d_{k+2} f_{i-k+1} (i-k+1) + 2 S_3 \sum_{k=0}^{i} (k+1) d_{k+1} w_{i-k+3} (i-k+3)! \\
& - S_{19} L_x^2 \sum_{k=0}^{i} (k+1) h_{k+1} w_{i-k+1} (i-k+1) + S_{15} L_x^3 \sum_{k=0}^{i} (k+1) d_{k+1} f_{i-k} \\
& + (2S_{10} - S_{14}) L_x^2 \sum_{k=0}^{i} (k+1) d_{k+1} w_{i-k+1} (i-k+1) + S_6 L_x^4 \sum_{k=0}^{i} d_k \phi_{i-k} \\
& + S_{28} L_x^2 \sum_{k=0}^{i} (k+1) d_{k+1} w_{i-k+1} (i-k+1) + S_{25} L_x^3 \sum_{k=0}^{i} (k+1) d_{k+1} f_{i-k} \\
& - 2 S_5 L_x \sum_{k=0}^{i} (k+1) d_{k+1} f_{i-k+2} (i-k+2)! - S_{18} L_x^3 \sum_{k=0}^{i} (k+1) h_{k+1} f_{i-k} \\
& + (2S_9 + S_{16}) L_x^2 \sum_{k=0}^{i} (k+1) d_{k+1} \phi_{i-k+1} (i-k+1) + S_{10} L_x^2 \sum_{k=0}^{i} (k+2)! d_{k+2} w_{i-k} \\
& + (S_{22} + S_{27}) L_x^4 \sum_{k=0}^{i} h_k w_{i-k} + S_{29} L_x^4 \sum_{k=0}^{i} d_k w_{i-k} + S_4 L_x^4 \sum_{k=0}^{i} d_k w_{i-k} + \\
& + (2S_{10} - S_{14}) L_x^2 \sum_{k=0}^{i} d_k w_{i-k+2} (i-k+2)! - S_{19} L_x^2 \sum_{k=0}^{i} h_k w_{i-k+2} (i-k+2)! \\
& + S_{28} L_x^2 \sum_{k=0}^{i} d_k w_{i-k+2} (i-k+2)! + (S_{22} + S_{27}) L_x^4 \sum_{k=0}^{i} h_k w_{i-k} + S_{21} L_x^4 \sum_{k=0}^{i} h_k \phi_{i-k}
\end{aligned}$$

$$+ S_{29}L_x^4\sum_{k=0}^{i} d_k w_{i-k} + S_4 L_x^4\sum_{k=0}^{i} d_k w_{i-k} - S_{18}L_x^3\sum_{k=0}^{i} h_k f_{i-k+1}(i-k+1)$$

$$+ (S_{15}-S_8)L_x^3\sum_{k=0}^{i} d_k f_{i-k+1}(i-k+1) + S_{25}L_x^3\sum_{k=0}^{i} d_k f_{i-k+1}(i-k+1)$$

$$+ S_9 L_x^2\sum_{k=0}^{i} d_k \phi_{i-k+2}(i-k+2)! + S_{16}L_x^2\sum_{k=0}^{i} d_k \phi_{i-k+2}(i-k+2)! + S_{26}L_x^4\sum_{k=0}^{i} d_k \phi_{i-k}$$

$$B_2^{(i)} = S_5\sum_{k=1}^{i} d_k w_{i-k+3}(i-k+3)! - S_1 L_x\sum_{k=1}^{i} d_k f_{i-k+2}(i-k+2)!$$

$$+ S_5\sum_{k=0}^{i}(k+1)d_{k+1}w_{i-k+2}(i-k+2)! + S_8 L_x^2\sum_{k=0}^{i}(k+1)d_{k+1}w_{i-k}$$

$$- S_1 L_x\sum_{k=0}^{i}(k+1)d_{k+1}f_{i-k+1}(i-k+1) - S_7 L_x^2\sum_{k=0}^{i}(k+1)d_{k+1}\phi_{i-k}$$

$$+ (S_8-S_{15})L^2\sum_{k=0}^{i} d_k w_{i-k+1}(i-k+1) + S_{18}L_x^2\sum_{k=0}^{i} h_k w_{i-k+1}(i-k+1)$$

$$- S_{25}L_x^2\sum_{k=0}^{i} d_k w_{i-k+1}(i-k+1) + S_{11}L_x^3\sum_{k=0}^{i} d_k f_{i-k} + S_{17}L_x^3\sum_{k=0}^{i} h_k f_{i-k}$$

$$+ S_{23}L_x^3\sum_{k=0}^{i} d_k f_{i-k} + (S_{13}-S_7)L_x^2\sum_{k=0}^{i} d_k \phi_{i-k+1}(i-k+1).$$

References

[1] J.N. Reddy, *Theory and Analysis of Elastic Plates*, Taylor & Francis, Philadelphia, PA, 1999.

[2] C.M. Wang, J.N. Reddy, K.H. Lee, *Shear Deformable Beams and Plates; Relationships with Classical Solution*, Elsevier, Amsterdam, 2000.

[3] N.F. Hanna, A.W. Leissa, A higher order shear deformation theory for the vibration of thick plates, *Journal of Sound and Vibration* 170 (1994) 545–555.

[4] J.L. Doong, Vibration and stability of an initially stressed thick plate according to a higher order deformation theory, *Journal of Sound and Vibration* 113 (1987) 425–440.

[5] J.N. Reddy, N.D. Phan, Stability and vibration of isotropic, orthotropic and laminated plates according to a higher-order shear deformation theory, *Journal of Sound and Vibration* 98 (1985) 157–170.

[6] H. Matsunga, Free vibration and stability of thick elastic plates subjected to in-plane forces, *Journal of Solids and Structures* 31 (1994) 3113–3124.

[7] K.M. Liew, C.M. Wang, Y. Xiang, S. Kitipornchai, *Vibration of Mindlin Plates*, Elsevier, Amsterdam, 1998.

[8] D.J. Dawe, S. Wang, Vibration of shear-deformable beams, plates using spline representations of deflection, shear strains, *International Journal of Mechanical Sciences* 36 (1994) 469–481.

[9] I. Shufrin, M. Eisenberger, Stability and vibration of shear deformable plates — first order and higher order analyses, *International Journal of Solids and Structures* 42 (2005) 1225–1251.

[10] B. Singh, V. Saxena, Transverse vibration of a rectangular plate with bidirectional thickness variation, *Journal of Sound and Vibration* 198 (1996) 51–56.

[11] M.S. Nerantzaki, J.T. Katsikadelis, An analog equation solution to dynamic analysis of plates with variable thickness, *Engineering Analysis with Boundary Elements* 17 (1996) 145–152.
[12] T. Mikami, J. Yoshimura, Application of the collocation method to vibration analysis of rectangular Mindlin plates, *Computer & Structures* 18 (1984) 425–431.
[13] G. Aksu, S.A. Al-Kaabi, Free vibration analysis of mindlin plates with linearly varying thickness, *Journal of Sound and Vibration* 119 (1987) 189–205.
[14] S.A. Al-Kaabi, G. Aksu, Free vibration analysis of mindlin plates with parabolically varying thickness, *Computer & Structures* 33 (1989) 1417–1421.
[15] T. Mizusawa, Vibration of rectangular mindlin plates with tapered thickness by the spline strip method, *Computer & Structures* 44 (1993) 451–463.
[16] Y.K. Cheung, D. Zhou, Vibration of tapered mindlin plates in terms of static timoshenko beam functions, *Journal of Sound and Vibration* 260 (2003) 693–709.
[17] A.D. Kerr, An extended Kantorovich method for the solution of eigenvalue problem, *International Journal of Solids and Structures* 15 (1969) 559–572.
[18] M. Eisenberger, A. Alexandrov, Buckling loads of variable thickness thin isotropic plates, *Thin-Walled Structures* 41 (9) (2003) 871–889.
[19] M. Eisenberger, Dynamic stiffness matrix for variable cross-section Timoshenko beams, *Communications in Numerical Methods in Engineering* 11 (1995) 507–513.
[20] M. Eisenberger, An exact high order beam element, *Computers & Structures* 81 (2003) 147–152.